

地球内核各向异性结构成因：矿物学模型和动力学机制

何宇,孙士川,徐云帆,李和平

中国科学院 地球化学研究所,中国科学院 地球内部物质高温高压重点实验室,贵阳 550081

摘要: 地震学观测表明,地球内核具有复杂的不均一性和各向异性结构,认知内核结构的关键在于研究内核各向异性结构的矿物学组成和动力学机制。本文将介绍内核各向异性结构特征,并探讨其矿物模型和动力学机制。在内核温压下,六方相(hcp)和体心立方(bcc)相铁合金都表现出各向异性,若其快轴沿自转轴产生定向排布,则可以解释内核南北方向快、赤道方向慢的各向异性特征。轻元素的加入将显著改变铁合金的各向异性,特别是超离子态铁-氢合金的快轴方向随氢含量的增加而发生倒转。内核各向异性的动力学机制可分为3种:①凝固时晶体的定向生长。凝固时的组构在内核温度下会很快消失,因此该机制不是导致内核各向异性结构的主要原因;②外应力驱动。外应力驱动的定向排列需要考虑内核物质的流变机制,目前的模型主要基于刚性内核假设,要求内核主要发生位错蠕变且黏度大于 10^{18} Pa·s;③扩散内应力驱动。若内核处于超离子态,地磁场驱动轻元素定向扩散所产生的内应力可驱动晶格的定向排布。上述机制的驱动力(化学对流、热对流、地磁场)均来自外核,因此了解外核动力学与内核动力学的相互作用是认知内核组成和结构的关键。

关键词: 地球内核;各向异性;高温高压;铁合金;定向排布

中图分类号: O521.2;P57 doi: 10.19658/j.issn.1007-2802.2023.42.100

The origin of anisotropic structure of the Earth's inner core from mineralogical model to dynamic mechanism

HE Yu, SUN Shi-chuan, XU Yun-fan, LI He-ping

CAS Key Laboratory of High-Temperature and High-Pressure Study of the Earth's Interior, Institute of Geochemistry, Chinese Academy of Sciences, Guiyang 550081, China

Abstract: Seismological observations suggested that Earth's inner core presents complex heterogeneity and anisotropic structure. The key to understand the structure of Earth's inner core is to study the mineralogical composition and dynamic mechanism of the anisotropic structure of Earth's inner core. Hexagonal close-packed (hcp) and body centered cubic (bcc) Fe alloys both have seismically anisotropic features under temperature and pressure conditions of the Earth's inner core. When the fast axis can be oriented along the Earth's rotation axis, the anisotropic characteristics of the Earth's inner core, which is fast in the north-south direction and slow in the equatorial direction, can be explained. The input of light elements into Fe alloys significantly changed the anisotropy of Fe alloys. Particularly, the fast axis orientation of superionic Fe-H alloys had changed inversely with the increase of H contents in those alloys. Under There are 3 kinds of dynamic mechanisms of the Earth's inner core. (1) The lattice preferred orientation (LPO) during the solidification period. The LPO texture and structure formed in the solidification process cannot be maintained at the temperature of Earth's inner core for a long time, therefore the LPO is not the main reason resulted in the

收稿编号:2023-131,2023-6-12 收到,2023-7-24 改回

基金项目:国家自然科学基金资助项目(42074104)

第一作者简介:何宇(1985—),男,博士,获第19届侯德封奖,研究方向:高温高压下地球内部物质性质的计算模拟研究. E-mail:heyu@mail.gyig.ac.cn.

引用此文:

何宇,孙士川,徐云帆,李和平. 2024. 地球内核各向异性结构成因:矿物学模型和动力学机制. 矿物岩石地球化学通报, doi: 10.19658/j.issn.1007-2802.2023.42.100

He Y, Sun S C, Xu Y F, Li H P. 2024. The origin of anisotropic structure of the Earth's inner core from mineralogical model to dynamic mechanism. Bulletin of Mineralogy, Petrology and Geochemistry, doi: 10.19658/j.issn.1007-2802.2023.42.100

anisotropic structure of the Earth's inner core; (2) The LPO due to the external stress: The directional arrangement driven by external stress needs to consider the rheological mechanism of the material in the Earth's inner core, while the current model is mainly established based on the assumption of a rigid inner core of the Earth. It is required that the dislocation creep mainly occurred in the Earth's inner core with the viscosity of its material exceeding to 10^{18} Pa·s. (3) The LPO due to the diffusion induced stress: If the Earth's inner core was under the superionic condition, the directional diffusion of light elements driven by the geomagnetic field could result in the presence of the lattice internal stress which would then result in the LPO. The driving forces of the above mechanisms (chemical convection, thermal convection, and geomagnetic field) are all sourced from the Earth's outer core. In this case, understanding the interaction mechanism between the Earth's outer core dynamics and the Earth's inner core dynamics is the key for understanding the composition and structure of the Earth's inner core.

Key words: Earth's inner core; anisotropy; high temperature and high pressure; iron alloys; lattice preferred orientation

0 引言

1936年,丹麦女科学家Inge Lehmann首次发现了地核中存在另一个地震波反射界面,并指出液态地核内部还存在一个固态的内核(Lehmann, 1936)。地球内核位于地球的最内层,其半径为1227.5 km(Kennett et al., 1995),相当于月球半径的70%。内核处于极端高温高压环境,其压强为330~364 GPa,温度为5000~6000 K,极端高温高压环境为认知内核的物质组成与结构带来了极大的困难。Birch(1940)首次从矿物学角度给出了内核是固态的证据,并认为无论内核还是外核,均含有一定的轻元素(Birch, 1952)。碳、氢、氧、硫、硅被认为是最有可能存在于地核的轻元素(Poirier and Shankland, 1993; Hirose et al., 2021; 刘锦等, 2022),然而对于轻元素的组成和含量目前尚无定论。

关于组成内核铁合金的晶体结构问题也存在争议。高压实验表明,在内核压力下,纯铁以六方密排(hcp)结构稳定存在(Mao et al., 1990, 1998),随后的理论计算也证明了hcp结构在内核温压下的稳定性(Vočadlo et al., 2000)。然而,在接近内核温度时,理论计算表明体心立方(bcc)结构更加稳定(Vočadlo et al., 2003; Belonoshko et al., 2003, 2017, 2021)。虽然近期的实验在接近内核的温度压力下都仅观察到稳定hcp结构铁合金(Tateno et al., 2010, 2012; Sakai et al., 2011; Turneaure et al., 2020),但这些实验的温度或压力仍然低于内核边界(ICB)条件,而理论计算表明bcc结构通常只能在接近熔化温度时才能稳定存在,在最近的液态铁凝固计算模拟中也发现了在内核压力下铁在凝固过程中先生成了bcc相,然后再生成了hcp相(Sun et al., 2022)。可见,确定内核稳定的铁合金结构,需要在接近铁熔化时的温度进行实验测量,而这显然极具挑战。

尽管无法直接获得来自地核的样品,然而地震波

却可以穿过地核,增进人们对其结构和性质的认知。地震学观测显示,地球内核表现出复杂的不均一和各向异性特征:包括地震波沿自转轴方向与沿赤道面方向的各向异性、各向异性随深度变化、波速和各向性的东西差异,以及内核结构的时变特征等。

复杂的不均一性和各向异性结构给认知内核的物质组成和动力学过程带来了困难,这与外核的均一性和各向同性特征存在矛盾,难以理解为何均一的外核物质固化后能形成的各向异性内核?其外在的驱动力是什么?有趣的是,内核各向异性与偶极地磁场均表现出柱对称结构,两者是否有某种联系?上述问题的解决,对于认知内核结构、物质组成和动力学过程至关重要。并且,认知内核结构与地磁场的关系将为理解地磁场的运行机制和与演化提供关键线索。本文将介绍内核各向异性结构特征,并探讨其矿物模型和动力学机制。

1 内核复杂的不均一性与各向异性特征

地震学的观测证实了地球内核的各向异性,前人已对内核结构及其各向性的地震学研究进行了系统性总结(Song, 1997; Deguen, 2012; Deuss, 2014; Tkalcic, 2015; 温联星等, 2018),这里主要是结合最新的研究结果进行概述。

1.1 压缩波速各向异性

内核各向异性首先被Poupinet等(1983)观测到,并发现地震压缩波(PKIKP)走时沿极轴方向比沿赤道面方向短。Morelli等(1986)明确了内核的各向异性,并指出内核各向异性呈现柱对称性,且快轴方向与自转轴方向一致,各向异性强度约为1%。同年,Woodhouse等(1986)发现,内核各向异性模型可以解释地球自由振荡中异常简正振型分裂的观测结果。后续的研究工作进一步证实了内核的各向异性(Creager, 1992; Song and Helmberger, 1993; Tromp, 1993; Su and

Dziewoński, 1995; Deuss et al., 2010), 估计的各向异性强度为1%~3%。不同的工作中其拟合的快轴方向与自转轴方向呈4~10°的夹角,但在近期的研究中却没有观测到各向异性对称轴与自转轴之间存在夹角(Irving and Deuss, 2011; Frost and Romanowicz, 2019)。Brett和Deuss(2020)在最近的研究中增加更多高纬度台站的压缩波走时数据,并对地幔的不均一性影响进行了修正,修正后的数据显示内核总体的各向异性在1.9%~2.3%,这与自由振荡的观测值一致(Tromp, 1993)。

1.2 各向异性随深度变化

通过利用不同震相的走时差,可以对内核不同深度的各向异性进行研究。研究发现在表面存在深度约100 km的各向同性层(Song and Helmberger, 1995; Niu and Wen, 2001; Yu and Wen, 2007; Waszek and Deuss, 2011等),在各向同性层还表现出明显的地震波衰减(Wen and Niu, 2002; Cao and Romanowicz, 2004; Yu and Wen, 2007; Waszek and Deuss, 2013等)。随着深度的增加,内核自转轴与赤道面方向的各向异性增强,而沿赤道面方向的地震波速最慢(Creager, 1992; Sun and Song, 2008a; Irving and Deuss, 2011等)。在内核最中心还存在一个厚度为300~700 km的最内核,其各向异性结构发生了明显变化,地震传播最慢方向从平行与赤道方向转移至了与自转轴方向呈约45~55°夹角(Ishii and Dziewoński, 2002, 2003; Beghein and Trampert, 2003; Sun and Song, 2008a, 2008b; Niu and Chen, 2008; Romanowicz et al., 2016; Stephenson et al., 2021; Pham and Tkalcic, 2023等)。最近,Pham和Tkalcic(2023)利用新增地震台站的数据,确认了半径为650 km最内核的存在,波速慢轴与自转轴夹角约50°,相应的波速比快轴(自转轴)方向低4%。有趣的是,Wang等(2015)利用尾波干涉方法发现,最内核可能存在赤道面的各向异性,或许最内核还存在一个平行于赤道面的快轴。

1.3 东西半球差异

内核结构在东西半球存在明显的不均一性和不同程度各向异性,PKiKP-PKIKP走时残差显示,在内核顶部约100 km处,东半球各向同性波速比西半球快约0.8%(Niu and Wen, 2001; Garcia, 2002; Waszek and Deuss, 2011)。半球的边界位置在不同的研究中有着显著的区别,通常东部边界在11°E至60°E之间,西部边界在-161°W到-180°W之间(Irving and Deuss, 2011; Waszek and Deuss, 2011)。东西半球波速的差异随着深度的增加而减小,在深度大于150 km处,东西半球的差异主要表现为各向异性的区别,表现为西半球的各向异性更强,东半球各向异性较弱(Tanaka

and Hamaguchi, 1997; Creager, 1999; Garcia and Souriau, 2000; Wen and Niu, 2002; Oreshin and Vinnik, 2004; Yu and Wen, 2006; Irving and Deuss, 2011; Lythgoe et al., 2014; Brett and Deuss, 2020)。

1.4 剪切波波速各向异性

除了压缩波,探测内核中的剪切波速也是认知内核结构的重要手段。由于内核边界处弱的压缩波到剪切波转化效率,以及内核中剪切波衰减,因而内核的剪切波震相(比如PKJKP)很难被直接观测到。尽管如此,更多的工作开始利用剪切波研究内核性质,证实了内核的固态属性。研究内核的剪切波各向异性却极具挑战,Wookey和Helffrich(2008)利用高密度精密台阵提取PKJKP震相,首次研究了内核的剪切波各向异性,并估计内核剪切波各向异性强度为1%。最近,Wang和Tkalcic(2021)利用地震尾波干涉的方法研究了剪切波在内核中的各向异性,剪切波沿着柱对称体倾斜角度方向的波速较慢,各向异性强度约为0.8%,这与自由振荡估算的内核剪切波各向异性强度基本一致(Tromp, 1993; Beghein and Trampert, 2003)。

1.5 内核结构时变特征

内核的时变特征最早由Song和Richards(1996)观察到,他们发现通过内核同一区域的地震波速在几十年的时间内就发生了显著变化。Zhang等(2005)进一步利用高质量的重复地震数据无可争议的证实了内核的时变现象。结合地球发电机的模拟结果(Gubbins, 1981; Glatzmaiers and Roberts, 1995),这种结构的时变特征被认为是内核相对于地幔的差速旋转引起,然而不同地震观测获得的内核差速旋转速度却差别很大,其数值变化从每年几度到每百万年几度(Song and Richards, 1996; Vidale et al., 2000; Song and Poupinet, 2007; Waszek et al., 2011; Yang and Song, 2020)。最近的观测中发现在2009年后这种差速旋转几乎停止了(Yang and Song, 2023)。杨翼和宋晓东(2021)对内核的时变特征进行了系统梳理和总结。

2 矿物学模型

内核温压条件下,实验研究铁合金的各向异性难度很大,而基于密度泛函理论的分子动力学模拟可以精确的描述内核温压下原子间相互作用,通过计算弹性系数,实现铁合金地震波速各向异性的计算研究。

2.1 六方密堆积(hcp)结构

hcp结构铁合金能够在较宽的温度和压力下稳定存在,因而其弹性各向异性被广泛的研究。Stixrude和Cohen(1995)首先在静态下计算了hcp纯铁的弹性各向异性,发现其存在较强的弹性各向异性,若其形成定

向排布,能够解释地震学观测到的内核地震波速异常。随着第一性原理分子动力学(AIMD)的发展,人们发现hcp铁的晶胞参数随着温度发生变化,在接近熔化温度时, c/a 值逐渐趋近于理想值(1.633),并伴随着弹性各向异性的减弱,因此 c/a 值成为判断hcp铁合金各向异性程度的重要标准(Steinle-Neumann et al., 2001; Gannarelli et al., 2005; Vočadlo et al., 2009)。在接近内核温压条件的高温高压实验中(Tateno et al., 2010),在330 GPa和5000 K的条件下,测量 c/a 值为1.6,这与Gannarelli等(2005)和Modak等(2007)的理论计算值吻合。Sun等计算的hcp-Fe在360 GPa和6000 K下的 c/a 值为1.609,表明内核温压下 c/a 小于理想值,hcp铁合金具有显著弹性各向异性,且压缩波沿c轴方向速度较快,考虑到内核的柱对称特性,将c轴方向与自转轴平行能够解释内核的南北极方向与赤道面方向的各向异性。

2.2 体心立方(bcc)结构

Belonoshko等(2007, 2008)与Vočadlo等(2009)计算了bcc铁的弹性系数,发现bcc铁的各向异性比hcp铁更强,压缩波沿[111]方向传播速度最快。Mattesini等(2010)将[111]轴平行于极轴方向,并以[111]轴为柱对称轴,构建平均的bcc组构模型,解释地震学观测到的内核各向异性。Mattesini等(2013)还考虑hcp和bcc两相共存的定向排布模型,可以解释内核的各向异性以及各向异性的东西半球差异。

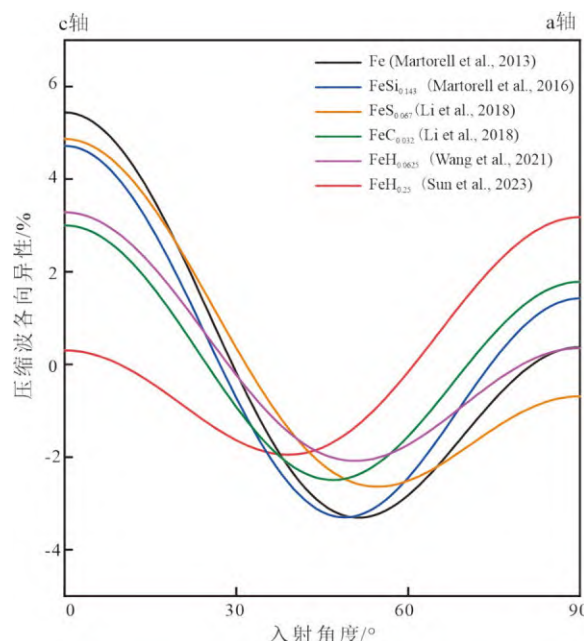
2.3 轻元素影响

地核密度比纯铁低,表明存在一定量的轻元素,然而对轻元素存在对于铁合金地震波速各向性的研究还很少。近期,第一性原理计算研究发现,六方相Fe-H、Fe-C和Fe-O合金在内核温压下转变成超离子态(He et al., 2022)。在超离子态合金中,这些轻元素像液体一样在铁的晶格中流动,导致了地震波速的降低,解释了内核低剪切波速特征。内核处于超离子态而非传统认知的固态,这是对于内核物态的全新认知。Sun等(2023)进一步计算了超离子态Fe-H(hcp)合金的压缩波波速各向异性,发现温度与H的含量都对Fe-H合金的波速各向异性产生显著影响,在360 GPa下,随着温度升高,Fe-H合金的各向异性先降低后增加,并伴随着波速快轴从c轴到a轴的转换。H含量的增加也有类似规律,因而FeH_{0.25}其在内核温压下波速沿a轴方向传播最快。依据前人计算的hcp相Fe(Martorell et al., 2013)、Fe-Si(Martorell et al., 2016)、Fe-S(Li et al., 2018)、Fe-C(Li et al., 2018)和Fe-H(Wang et al., 2021; He et al., 2022)合金在内核温压下的弹性系数,我们利用Christoffel方程(Anderson, 1989)计算

了上述铁合金沿c轴方向到a轴方向的压缩波速变化,并利用该方向平均波速对数据进行了归一化处理。如图1所示,轻元素杂质降低了hcp铁合金压缩波波速各向异性,其中Si与S仅导致各向异性轻微减小,而C与H对各向异性的影响明显,特别是FeH_{0.25}的各向异性与其他铁合金有明显的不同,其中地震波沿a轴方向传播最快。可见,轻元素的种类和含量对于hcp相铁合金的波速各向异性有明显影响,这与轻元素掺杂对hcp铁的 c/a 比的影响有关(Sun et al., 2023)。对于超离子态Fe-H合金,H含量增加导致快轴倒转,将直接影响与地震学观测数据匹配时的晶体排布方向,需要将a-b平面方向(考虑到hcp结构的对称性)与地球自转轴平行以满足地震学观测到的南北方向快、赤道面方向慢的内核结构特征。

3 动力学机制

地震波速各向异性通常来源于晶格的定向排布(lattice preferred orientation, LPO)或是具有不同弹性性质的两相物质形成定向的形状排布(shape preferred orientation, SPO)。内核条件下,hcp和bcc结构铁合金均表现处明显的弹性各向异性,因而内核晶体的定向排列解释内核各向异性成因被广泛研究并讨论。



入射角度0°对应[001](c轴)方向,入射角度90°对应[100]方向。超离子态FeH_{0.25}的快轴沿a轴方向,表现出与其他合金各向性的显著差别

图1 内核温压下Fe、Fe-Si、Fe-S、Fe-C和Fe-H的压缩波波速(V_P)随着入射角度在(010)平面上的变化

Fig.1 Variations of compressional velocities (V_P) in Fe, Fe-Si, Fe-S, Fe-C, and Fe-H alloys with changes of propagation directions (incident angles) on the (010) plane

Singh等人(2000)提出内核各向异性的定向形状排布机制,认为内核各向异性由分散于固态内核中,沿赤道面定向排布的非球形液体相导致。可见,无论是晶体或形状的定向排布均能构建各向异性模型,而认知各向异性起因的关键在于了解内核中晶体或形状定向排布的驱动力,即内核各向异性结构形成的动力学机制(表1)。

3.1 凝固过程中的定向排列机制

Karato(1993)认为,内核凝固时铁合金仍会保有一定的磁性,并在地磁场的作用下形成各向异性的结构。凝固时,晶体定向枝晶生长也可以导致晶体定向排列,Bergman(1997)认为在外核中热传导的不均匀性可以导致凝固时铁合金沿赤道方向的定向生长,并形成圆柱对称性的各向异性结构。该结构可以解释观测到的地震波速和衰减各向异性。然而,近期实验研究表明,这种因凝固而形成的各向异性结构经过几天的高温退火就会消失(Bergman et al., 2010)。因此,因凝固而形成的各向异性结构无法在内核条件下长期存在,该种机制无法解释内核深部的各向异性结构。

3.2 外应力驱动机制

若外应力作用导致内核物质发生位错蠕变,可以形成各向异性结构,相反,如果仅发生扩散蠕变则不能形成各向异性结构。因而对于内核条件下矿物的流变性质的研究对于认知内核各向异性形成十分重要,然而蠕变机制并非仅取决于物质的本征性质,还与外应力大小和作用方式有关,这使得该问题的研究变得非常复杂,而目前的研究也基于其在流变过程中能够形成晶体定向排布的假设。

内核的热对流最早被Jeanloz and Wenk(1988)提出解释内核各向异性,然而基于目前已知的内核高热导率并不支持内核产生显著的热对流。然而,基于内核边界不均匀的热分布,将会导致内核边界凝固速率的差异,甚至在内核边界某些区域可能发生熔化。当内核边界相变速率大于内核流变速率时,会导致内核物质的横向平移,即物质在一边半球凝固,在另一个边半球熔化,物质从凝固半球平移至熔化的半球(Alboussière et al., 2010; Monnereau et al., 2010)。若内核西半球发生凝固,东半球发生熔化,根据东西半球不同的

表1 内核动力学模型

Table 1 Dynamic models for the Earth's inner core

机制	驱动力	基本原理	适用性	局限性	参考文献
内核凝固时晶体 定向增长	地磁场产生的电磁力	地磁场导致内核凝固时铁合金晶体择优排布	提供了一个潜在的各向异性成因	凝固时的择优排布无法长时间保持	Karato, 1993
	外核对流动力	外核对流导致的内核各向异性枝晶生长	解释各向异性及各向异性随深度变化	凝固时的择优排布无法长时间保持	Bergman, 1997
热力		热对流导致择优排布	解释两极和赤道的各向异性	目前认为内核热导率很高, 无法驱动晶格定向排布	Jeanloz and Wenk, 1988; Romanowicz et al., 1996
		受到核幔边界不均匀热流通过外核作用于内核的凝固过程, 导致了东西半球不同的凝固过程	解释了内核浅部东西半球波速差异	无法解释内核深部的各向异性	Aubert et al., 2008
外应力驱动		西半球内核凝固, 东半球内核熔化, 西半球晶体向东半球迁移, 导致东西半球差异	解释外核底部的低速层成因和内核浅部东西半球波速差异	模型要求较高粘度($>10^{18}$ Pa·s)	Alboussière et al., 2010; Monnereau et al., 2010
	外核对流动力	外核对流导致的赤道面优先沉积, 并且沉积后的物质向两极对流	解释两极和赤道地震波速各向异性	无法解释东西半球波速各向异性差异与最内核各向异性成因。	Yoshida et al., 1996; Deguen et al., 2011
	外核对流动力及热力	同时考虑赤道面的优先生长和西半球晶体向东半球迁移	通过优化参数, 解释了两极和赤道地震波各向异性; 各向异性随深度变化; 东西半球波速和各向异性差异	模型要求较高粘度($>10^{18}$ Pa s)	Frost et al., 2021
地磁场产生的电磁力		地磁场Maxwell力导致择优排布	提供了一个潜在的各向异性成因	该模型下六方铁c-轴沿赤道方向排布, 无法解释两极和赤道方向地震波速各向异性	Karato, 1999; Buffett and Wenk, 2001
		地球磁场产生的焦耳热驱动内核晶体择优排布	提供了一个潜在的各向异性成因	缺乏与地球内核地震学观测结果对比	Takehiro, 2011
内应力驱动	地磁场产生的电磁力	电磁力作用下的氢离子扩散导致晶驱动晶格定向排布	解释了两极和赤道地震波各向异性; 各向异性随深度变化	要求内核中有较高的氢含量(约0.44%)	Sun et al., 2023

晶粒尺寸就可以解释地震学观测到的内核东西半球地震波速和衰减的差异。然而,这个模型需要内核保持一定的刚性(黏度>10¹⁸ Pa·s),这个值显著高于目前地球物理观测和高温高压计算模拟估计的内核黏度(Koot and Dumberry, 2011; Belonoshko et al., 2019; Ritterbex and Tsuchiya, 2020)。另外,该模型本身并不能解释南北方向与赤道面方向的地震波速各向异性,即使考虑凝固时形成了某些定向排布组织,其也会在其平移过程中逐渐消失(Bergman et al., 2010)。

考虑到热对流无法形成各向异性结构的困境,Yoshida等(1996)提出了内核弛豫模型,他们认为内核结晶过程与外核对流是耦合的,并在内核边界表现出不均一的凝固过程。据此,他们提出在外核旋转对流过程中,内核在赤道面区域的生长速度将大于其他方向,从而形成由赤道面到两极的物质流动,以保持内核边界静水压一致。内核边界的对流产生的应力场,导致了内核晶体的定向排布,从而解释了内核各向异性。他们估计若内核黏度为10²¹ Pa·s,形成该各向异性结构需要几十亿年的时间,而若内核黏度更低,则需要花费更多的时间。Deguen等(2011)指出,对流可以导致内核分层,并解释内核的各向同性表层。近期,Frost等(2021)将该模型与上面提到了内核东西半球平移模型结合,在刚性内核(黏度>10¹⁸ Pa·s)与内核东西平移速率低于结晶速率的前提下,可以产生由西向东与由赤道面向两极的较强应力场。考虑到应力导致hcp铁合金位错蠕变形成<c+a>各向异性组织,能够很好的解释地震学观测到的内核各向异性特征。

地球发电机模拟表明内核边界存在沿自转轴方向(B_P)和环绕内核方向(B_T)的两个磁场分量。Karato(1999)考虑了由 B_T 分量在内核边界产生的Maxwell应力作用,该应力大小随着纬度变化,从而产生了轴向对称应力差,从而导致hcp铁合金的c轴与自转轴平行。Buffett和Bloxham(2000)进一步考虑了内核在化学和热平衡状态下的Maxwell应力作用,并发现 B_T 分量产生的应力会被浮力抵消,因而无法深入作用与内核深处,仅依靠 B_T 分量导致的应力不足以产生显著的各向异性结构。Buffett和Wenk(2001)进一步考虑了 B_P 和 B_T 两个分量产生的Maxwell应力,并发现两个分量的作用下,沿水平方向的合力不受内核热平衡影响,从而可以导致形成hcp铁的c轴方向垂直于自转轴的定向排列。然而,这要求地震波速沿hcp铁合金c轴方向速度更慢时,相关模型才能够符合地震学观测。

3.3 扩散内应力驱动机制

在超离子态Fe-H合金中,H离子可以在晶格中快速扩散,其在扩散区域的扩散流J可由广义Fick定律表达

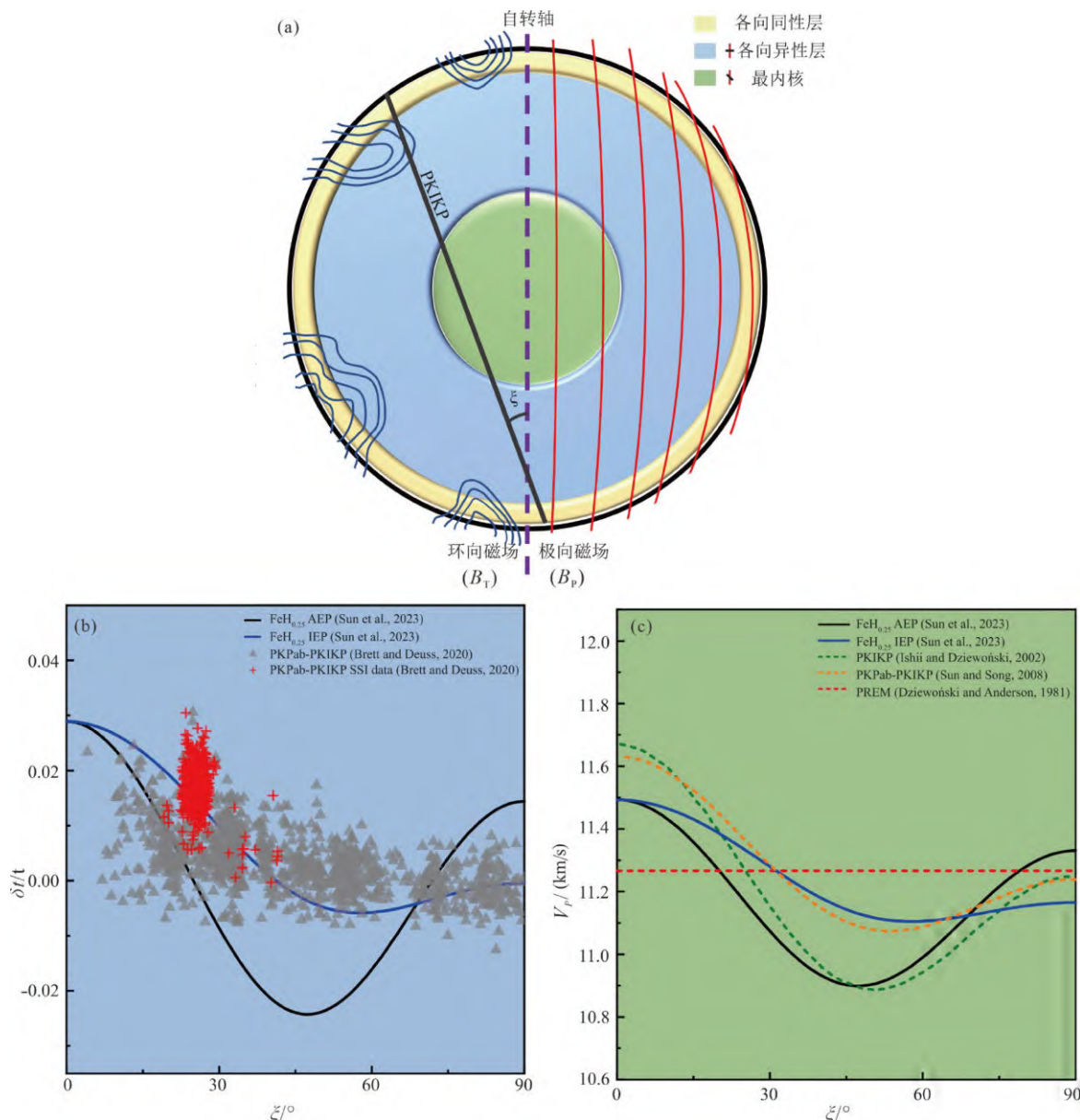
$$J_H = -D_H \frac{\partial \mu_H}{\partial x} \quad (1)$$

式中, D 是H离子的扩散系数, μ 是H离子的化学势。因此,在外应力的作用下体系变形可以导致离子化学势的改变。外应力作用下的扩散可以导致晶界或晶格扩散,即蠕变。因此,也将应力导致的离子扩散现象称为“应力扩散”(stress-induced diffusion, SID)。相应的,离子扩散也可以在晶格内部产生的内应力场,称为“扩散应力”(diffusion-induced stress, DIS; 陈永翀等, 2006)。

Sun等(2023)研究了hcp相Fe-H合金的扩散性质,发现H离子沿c轴方向扩散更为有利。他们利用人工智能驱动的科学新方法(AI for Science)实现了外电场下大规模分子动力学模拟,并发现c轴方向与电场方向平行排布时体系能量最有利。因此,他们提出偶极地磁场作用下氢离子可以发生各向异性扩散,并在体系中产生内应力,由于内核所处的高温高压环境,在内应力的驱动下导致晶格的定向排布,使得c轴方向与内核的电场方向一致。基于此机理,可以建立地磁场驱动下的内核各向异性模型。基于地球发电机数值模拟结果,外核动力学过程产生的磁场将在内核边界(ICB)处分解为环向地磁场 B_T 和极向地磁场 B_P 两个分量。偶极地磁中极向磁场 B_P 能够穿透整个内核,而环向磁场由于趋肤效应的存在,只能扩散到内核顶部较浅的区域(图2a黄色区域)。在内核顶部处,由 B_T 和 B_P 的共同作用下,将不会形成显著的各向异性组织,从而解释了内核浅部的各向同性层。在深部, B_P 将起到主导作用,根据安培定律,相应的电流方向将垂直于 B_P 方向。如上所述,超离子态铁-氢合金c轴平行于电流方向排布对体系能量最为有利。根据此全新机理,可以构建地磁场驱动下的超离子态内核模型,其c轴将与赤道面平行,从而导致与地震学观测结果一致的各向异性的地震波速(图2b)。若进一步考虑c轴在赤道面的各向异性排布,还可以解释最内核的各向异性结构变化(图2c)。值得注意的是,该工作建立了地球内核结构与地磁场的关系,或为地磁场的研究提供全新的研究思路和方法。

4 结论与展望

地震学观测表明地球内核表现出复杂的不均一性和各向异性。认知复杂内核结构的关键在于研究内核各向异性结构的成因,包括其矿物学组成和动力学机制。在内核温压下,无论是hcp还是bcc铁合金晶格定向排布(LPO)或是内核中存在形状定向排布(SPO)的液滴都可以形成各向异性结构。因而,驱动定向排布形成的动力学机制成为了研究重点。尽管凝固过程



(a) 内核中极向(B_p ;红色)和环向(B_T ;蓝色)的磁场分布,以及内核结构随深度的变化,包括内核表面的各向同性层(黄色区域),各向同性层下方南北快东西慢的各向异性层(蓝色区域)和位于最深处慢速方向与自转轴呈约45–55°夹角的最内核(绿色区域)。黑线是震相PKIKP在内核中的传播路径,其与自转轴的夹角为 ξ ;(b)蓝色区域波速随 ξ 的变化观测量(Brett and Deuss, 2020)与超离子态Fe-H各向异性模型对比(Sun et al., 2023),其中蓝色和黑色曲线为各向同性赤道面(IEP)与各向异性赤道面(AEP)模型;(c)最内核波速随 ξ 的变化观测量(Dziewoński and Anderson, 1981; Ishii and Dziewoński, 2002; Sun and Songa, 2008)与超离子态Fe-H各向异性模型对比(Sun et al., 2023)

图2 内核中地磁场示意图、随深度变化各向异性构造变化及超离子态内核模型与不同深度地震学观测对比

Fig.2 Schematic diagrams of geomagnetic field and depth-dependent anisotropic texture changes of the Earth's inner core, and comparison of the superionic Earth's inner core model with seismological observations at different depths

中晶格可以发生定向生长,然而在内核的温度下,凝固形成的各向异性结构无法长期保持,无法解释内核深部的各向异性结构。因而,内核的各向异性应来自于内核形成后外力的作用。目前主要考虑内外核边界化学对流、热和地磁场的不均一驱动作用。虽然不同的动力学机制都一定程度上解释了各向异性或不均一性成因,然而这些模型的成立都强烈依赖于内核参数的选择,比如黏度、铁合金的滑移系统、弹性性质、轻元素

种类或含量等,并且尚无一个模型能够完全解释目前已知的内核结构特征。

未来进展一方面取决于更多地震学观测数据,密集台阵的广泛布设有利于提取信噪比较低的地核震相。另外,大地震尾波干涉方法将提供更多的内核结构信息(Wang et al., 2015; Wang and Tkalcic, 2020; Tkalcic et al., 2020)。其中,赤道面各向异性特征,以及剪切波波速各向异性变化等关键信息将为区分内核

矿物与动力学模型提供更多制约条件。另一方面取决于内核温压下物质的实验与计算模拟研究:包括内核稳定的铁合金相的确定、内核轻元素的种类与含量、内核铁合金的热力学性质、弹性性质和流变性质的准确测量等。除此之外,解释内核之谜,还需要从地球系统科学的角度出发,系统考虑地球内核结构与地磁场的耦合作用,内核动力学与外核动力学的相互关系,以及核-幔相互作用(核幔边界的不均一性和热输运性质)对于地核的影响。可见地核动力学研究的突破需要地震学、地磁学、磁流体力学、高温高压矿物学、计算模拟等多学科交叉的合作研究。

作者贡献声明: 何宇,研究构思和设计、数据收集和整理、制图、撰写稿件;孙士川,数据整理和制图;徐云帆,数据统计并参与文章写作;李和平,文章写作与修订。

利益冲突声明: 作者保证本文无利益冲突。

参考文献 (References):

- Alboussière T, Deguen R, Melzani M. 2010. Melting-induced stratification above the Earth's inner core due to convective translation. *Nature*, 466: 744–747
- Anderson D L. 1989. Theory of the earth. Boston: Blackwell Scientific
- Aubert J, Amit H, Hulot G, Olson P. 2008. Thermochemical flows couple the Earth's inner core growth to mantle heterogeneity. *Nature*, 454(7205): 758–761
- Beghein C, Trampert J. 2003. Robust normal mode constraints on inner-core anisotropy from model space search. *Science*, 299(5606): 552–555
- Belonoshko A B, Ahuja R, Johansson B. 2003. Stability of the body-centred-cubic phase of iron in the Earth's inner core. *Nature*, 424(6952): 1032–1034
- Belonoshko A B, Fu J, Bryk T, Simak S I, Mattesini M. 2019. Low viscosity of the Earth's inner core. *Nature Communications*, 10(1): 2483
- Belonoshko A B, Fu J, Smirnov G. 2021. Free energies of iron phases at high pressure and temperature: Molecular dynamics study. *Physical Review B*, 104(10): 104103
- Belonoshko A B, Lukinov T, Fu J, Zhao J, Davis S, Simak S I. 2017. Stabilization of body-centred cubic iron under inner-core conditions. *Nature Geoscience*, 10(4): 312–316
- Belonoshko A B, Skorodumova N V, Davis S, Osipov A N, Rosengren A, Johansson B. 2007. Origin of the low rigidity of the earth's inner core. *Science*, 316(5831): 1603–1605
- Belonoshko A B, Skorodumova N V, Rosengren A, Johansson B. 2008. Elastic anisotropy of Earth's inner core. *Science*, 319(5864): 797–800
- Bergman M I, Lewis D J, Myint I H, Slivka L, Karato S I, Abreu A. 2010. Grain growth and loss of texture during annealing of alloys, and the translation of Earth's inner core. *Geophysical Research Letters*, 37(22): L22313
- Bergman M I. 1997. Measurements of electric anisotropy due to solidification texturing and the implications for the Earth's inner core. *Nature*, 389(6646): 60–63
- Birch A F. 1940. The alpha-gamma transformation of iron at high pressures, and the problem of the earth's magnetism. *American Journal of Science*, 238(3): 192–211
- Birch F. 1952. Elasticity and constitution of the Earth's interior. *Journal of Geophysical Research*, 57(2): 227–286
- Brett H, Deuss A. 2020. Inner core anisotropy measured using new ultra-polar PKIKP paths. *Geophysical Journal International*, 223(2): 1230–1246
- Buffett B A, Bloxham J. 2000. Deformation of Earth's inner core by electromagnetic forces. *Geophysical Research Letters*, 27(24): 4001–4004
- Buffett B A, Wenk H R. 2001. Texturing of the Earth's inner core by Maxwell stresses. *Nature*, 413(6851): 60–63
- Cao A, Romanowicz B. 2004. Hemispherical transition of seismic attenuation at the top of the earth's inner core. *Earth and Planetary Science Letters*, 228(3–4): 243–253
- 陈永翀,黎振华,其鲁,张永刚,陈昌麒. 2006. 固体中的扩散应力研究. 金属学报, 42(3): 225–233 [Chen Y C, Li Z H, Qi L, Zhang Y G, Chen C Q. 2006. Diffusion-induced stresses in solids. *Acta Metallurgica Sinica*, 42(3): 225–233 (in Chinese with English abstract)]
- Creager K C. 1992. Anisotropy of the inner core from differential travel times of the phases PKP and PKIKP. *Nature*, 356: 309–314
- Creager K C. 1999. Large-scale variations in inner core anisotropy. *Journal of Geophysical Research: Solid Earth*, 104(B10): 23127–23139
- Deguen R, Cardin P, Merkel S, Leinensohn R A. 2011. Texturing in Earth's inner core due to preferential growth in its equatorial belt. *Physics of the Earth and Planetary Interiors*, 188(3–4): 173–184
- Deguen R. 2012. Structure and dynamics of Earth's inner core. *Earth and Planetary Science Letters*, 333–334: 211–225
- Deuss A, Irving J C E, Woodhouse J H. 2010. Regional variation of inner core anisotropy from seismic normal mode observations. *Science*, 328(5981): 1018–1020
- Deuss A. 2014. Heterogeneity and anisotropy of earth's inner core. *Annual Review of Earth and Planetary Sciences*, 42(1): 103–126
- Dziewonski A M, Anderson D L. 1981. Preliminary reference Earth model. *Physics of the Earth and Planetary Interiors*, 25(4): 297–356
- Frost D A, Lasbleis M, Chandler B, Romanowicz B. 2021. Dynamic history of the inner core constrained by seismic anisotropy. *Nature Geoscience*, 14(7): 531–535
- Frost D A, Romanowicz B. 2019. On the orientation of the fast and slow directions of anisotropy in the deep inner core. *Physics of the Earth and Planetary Interiors*, 286: 101–110
- Gannarelli C M S, Alfè D, Gillan M J. 2005. The axial ratio of hexagonal close-packed iron at the conditions of the Earth's inner core. *Physics of the Earth and Planetary Interiors*, 152(1–2): 67–77
- Garcia R, Souriau A. 2000. Inner core anisotropy and heterogeneity level. *Geophysical Research Letters*, 27(19): 3121–3124
- Garcia R. 2002. Constraints on upper inner-core structure from waveform inversion of core phases. *Geophysical Journal International*, 150(3): 651–664
- Glatzmaier G A, Roberts P H. 1995. A three-dimensional self-consistent computer simulation of a geomagnetic field reversal. *Nature*, 377(6546): 203–209
- Gubbins D. 1981. Rotation of the inner core. *Journal of Geophysical Research: Solid Earth*, 86(B12): 11695–11699

- He Y, Sun S, Kim D Y, Jang B G, Li H, Mao H. 2022. Superionic iron alloys and their seismic velocities in Earth's inner core. *Nature*, 602(7896): 258–262
- Hirose K, Wood B, Vočadlo L. 2021. Light elements in the Earth's core. *Nature Reviews Earth & Environment*, 2: 645–658
- Irving J C E, Deuss A. 2011. Hemispherical structure in inner core velocity anisotropy. *Journal of Geophysical Research (Solid Earth)*, 116(B4): B04307
- Ishii M, Dziewoński A M. 2002. The innermost inner core of the earth: Evidence for a change in anisotropic behavior at the radius of about 300 km. *Proceedings of the National Academy of Sciences*, 99(22): 14026–14030
- Ishii M, Dziewoński A M. 2003. Distinct seismic anisotropy at the centre of the Earth. *Physics of the Earth and Planetary Interiors*, 140(1–3): 203–217
- Jeanloz R, Wenk H R. 1988. Convection and anisotropy of the inner core. *Geophysical Research Letters*, 15(1): 72–75
- Karato S L. 1999. Seismic anisotropy of the Earth's inner core resulting from flow induced by Maxwell stresses. *Nature*, 402(6764): 871–873
- Karato S. 1993. Inner Core Anisotropy Due to the Magnetic Field: Induced Preferred Orientation of Iron. *Science*, 262(5140): 1708–1711
- Kennett B L N, Engdahl E R, Buland R. 1995. Constraints on seismic velocities in the Earth from traveltimes. *Geophysical Journal International*, 122(1): 108–124
- Koot L, Dumbrerry M. 2011. Viscosity of the Earth's inner core: Constraints from nutation observations. *Earth and Planetary Science Letters*, 308(3–4): 343–349
- Lehmann I. 1936. P'. *Publ. Bur. Cent. Seismol. Int. A*, 14: 87–115
- Li Y, Vočadlo L, Brodholt J P. 2018. The elastic properties of hcp-Fe alloys under the conditions of the Earth's inner core. *Earth and Planetary Science Letters*, 493: 118–127
- 刘锦, 吕超甲, 赵超帅. 2022. 矿物高压稳定性与深部挥发分循环过程. *矿物岩石地球化学通报*, 41(2): 245–259, 202 [Liu J, Lyu C J, Zhao C S. 2022. High-pressure stability of minerals and volatiles cycling in the deep earth. *Bulletin of Mineralogy, Petrology and Geochemistry*, 41(2): 245–259, 202 (in Chinese with English abstract)]
- Lythgoe K H, Deuss A, Rudge J F, Neufeld J A. 2014. Earth's inner core: Innermost inner core or hemispherical variations? *Earth and Planetary Science Letters*, 385: 181–189
- Mao H, Shu J, Shen G, Hemley R J, Li B, Singh A K. 1998. Elasticity and rheology of iron above 220 GPa and the nature of the Earth's inner core. *Nature*, 396(6713): 741–743
- Mao H K, Wu Y, Chen L C, Shu J F, Jephcoat A P. 1990. Static compression of iron to 300 GPa and Fe_{0.8} Ni_{0.2} alloy to 260 GPa: Implications for composition of the core. *Journal of Geophysical Research: Solid Earth*, 95(B13): 21737–21742
- Martorell B, Vočadlo L, Brodholt J, Wood I G. 2013. Strong premelting effect in the elastic properties of hcp-Fe under inner-core conditions. *Science*, 342(6157): 466–468
- Martorell B, Wood I G, Brodholt J, Vočadlo L. 2016. The elastic properties of hcp-Fe 1-x Si x at Earth's inner-core conditions. *Earth and Planetary Science Letters*, 451: 89–96
- Mattesini M, Belonosko A B, Buorn E, Ramírez M, Simak S I, Udías A, Mao H K, Ahuja R. 2010. Hemispherical anisotropic patterns of the Earth's inner core. *Proceedings of the National Academy of Sciences*, 107(21): 9507–9512
- Mattesini M, Belonosko A B, Tkalcic H, Buorn E, Udias A, Ahuja R. 2013. Candy wrapper for the earth's inner core. *Scientific Reports*, 3(1): 2096
- Modak P, Verma A K, Rao R S, Godwal B K, Stixrude L, Jeanloz R. 2007. Stability of the hcp phase and temperature variation of the axial ratio of iron near Earth-core conditions. *Journal of Physics: Condensed Matter*, 19(1): 016208
- Monnereau M, Calvet M, Margerin L, Souriau A. 2010. Lopsided growth of Earth's inner core. *Science*, 328(5981): 1014–1017
- Morelli A, Dziewoński A M, Woodhouse J H. 1986. Anisotropy of the inner core inferred from PKIKP travel times. *Geophysical Research Letters*, 13(13): 1545–1548
- Niu F, Chen Q F. 2008. Seismic evidence for distinct anisotropy in the innermost inner core. *Nature Geoscience*, 1(10): 692–696
- Niu F, Wen L. 2001. Hemispherical variations in seismic velocity at the top of the Earth's inner core. *Nature*, 410(6832): 1081–1084
- Oreshin S I, Vinnik L P. 2004. Heterogeneity and anisotropy of seismic attenuation in the inner core. *Geophysical Research Letters*, 31(2): L02613
- Pham T S, Tkalcic H. 2023. Up-to-fivefold reverberating waves through the Earth's center and distinctly anisotropic innermost inner core. *Nature Communications*, 14(1): 754
- Poirier J P, Shankland T J. 1993. Dislocation melting of iron and the temperature of the inner core boundary, revisited. *Geophysical Journal International*, 115(1): 147–151
- Poupinet G, Pillet R, Souriau A. 1983. Possible heterogeneity of the Earth's core deduced from PKIKP travel times. *Nature*, 305(5931): 204–206
- Ritterbe S, Tsuchiya T. 2020. Viscosity of hcp iron at Earth's inner core conditions from density functional theory. *Scientific Reports*, 10(1): 6311
- Romanowicz B, Cao A M, Godwal B, Wenk R, Ventosa S, Jeanloz R. 2016. Seismic anisotropy in the Earth's innermost inner core: Testing structural models against mineral physics predictions. *Geophysical Research Letters*, 43(1): 93–100
- Romanowicz B, Li X, Durek J. 1996. Anisotropy in the inner core: Could it be due to low-order convection? *Science*, 274(5289): 963–966
- Sakai T, Ohtani E, Hirao N, Ohishi Y. 2011. Stability field of the hcp-structure for Fe, Fe-Ni, and Fe-Ni-Si alloys up to 3 Mbar. *Geophysical Research Letters*, 38(9): L09302
- Singh S C, Taylor M A J, Montagner J P. 2000. On the presence of liquid in earth's inner core. *Science*, 287(5462): 2471–2474
- Song X, Helmberger D V. 1993. Anisotropy of Earth's inner core. *Geophysical Research Letters*, 20(23): 2591–2594
- Song X, Helmberger D V. 1995. Depth dependence of anisotropy of Earth's inner core. *Journal of Geophysical Research: Solid Earth*, 100(B6): 9805–9816
- Song X, Poupinet G. 2007. Inner core rotation from event-pair analysis. *Earth and Planetary Science Letters*, 261(1–2): 259–266
- Song X, Richards P G. 1996. Seismological evidence for differential rotation of the Earth's inner core. *Nature*, 382(6588): 221–224
- Song X D. 1997. Anisotropy of the Earth's inner core. *Reviews of Geophysics*, 35(3): 297–313
- Steinle-Neumann G, Stixrude L, Cohen R E, Güleren O. 2001. Elasticity of iron at the temperature of the Earth's inner core. *Nature*, 413(6851): 57–

- 60
- Stephenson J, Tkalčić H, Cambridge M. 2021. Evidence for the innermost inner core: Robust parameter search for radially varying anisotropy using the neighborhood algorithm. *Journal of Geophysical Research: Solid Earth*, 126(1): e2020JB020545
- Stixrude L, Cohen R E. 1995. High-pressure elasticity of iron and anisotropy of earth's inner core. *Science*, 267(5206): 1972–1975
- Su W, Dziewonski A M. 1995. Inner core anisotropy in three dimensions. *Journal of Geophysical Research: Solid Earth*, 100(B6): 9831–9852
- Sun S, He Y, Yang J, Lin Y, Li J, Kim D Y, Li H, Mao H. 2023. Superionic effect and anisotropic texture in Earth's inner core driven by geomagnetic field. *Nature Communications*, 14(1): 1656
- Sun X, Song X. 2008. The inner inner core of the Earth: Texturing of iron crystals from three-dimensional seismic anisotropy. *Earth and Planetary Science Letters*, 269(1-2): 56–65
- Sun X, Song X. 2008. Tomographic inversion for three-dimensional anisotropy of Earth's inner core. *Physics of the Earth and Planetary Interiors*, 167(1-2): 53–70
- Sun Y, Zhang F, Mendelev M I, Wentzcovitch R M, Ho K M. 2022. Two-step nucleation of the Earth's inner core. *Proceedings of the National Academy of Sciences*, 119(2): e2113059119
- Takehiro S I. 2011. Fluid motions induced by horizontally heterogeneous Joule heating in the Earth's inner core. *Physics of the Earth and Planetary Interiors*, 184(3–4): 134–142
- Tanaka S, Hamaguchi H. 1997. Degree one heterogeneity and hemispherical variation of anisotropy in the inner core from *PKP* (BC)–*PKP* (DF) times. *Journal of Geophysical Research: Solid Earth*, 102(B2): 2925–2938
- Tateno S, Hirose K, Komabayashi T, Ozawa H, Ohishi Y. 2012. The structure of Fe - Ni alloy in Earth's inner core. *Geophysical Research Letters*, 39(12): L12305
- Tateno S, Hirose K, Ohishi Y, Tatsumi Y. 2010. The structure of iron in Earth's inner core. *Science*, 330(6002): 359–361
- Tkalčić H, Pham T S, Wang S. 2020. The Earth's coda correlation wavefield: Rise of the new paradigm and recent advances. *Earth-Science Reviews*, 208: 103285
- Tromp J. 1993. Support for anisotropy of the Earth's inner core from free oscillations. *Nature*, 366(6456): 678–681
- Turneaure S J, Sharma S M, Gupta Y M. 2020. Crystal structure and melting of fe shock compressed to 273 GPa: *In Situ* X-Ray diffraction. *Physical Review Letters*, 125(21): 215702
- Vidale J E, Dodge D A, Earle P S. 2000. Slow differential rotation of the Earth's inner core indicated by temporal changes in scattering. *Nature*, 405(6785): 445–448
- Vočadlo L, Alfè D, Gillan M J, Wood I G, Brodholt J P, Price G D. 2003. Possible thermal and chemical stabilization of body-centred-cubic iron in the Earth's core. *Nature*, 424(6948): 536–539
- Vočadlo L, Brodholt J, Alfè D, Gillan M J, Price G D. 2000. *Ab initio* free energy calculations on the polymorphs of iron at core conditions. *Physics of the Earth and Planetary Interiors*, 117(1-4): 123–137
- Vočadlo L, Dobson D P, Wood I G. 2009. *Ab initio* calculations of the elasticity of hcp-Fe as a function of temperature at inner-core pressure. *Earth and Planetary Science Letters*, 288(3-4): 534–538
- Wang S, Tkalčić H. 2020. Seismic event coda-correlation: Toward global coda-correlation tomography. *Journal of Geophysical Research: Solid Earth*, 125(4): e2019JB018848
- Wang S, Tkalčić H. 2021. Shear-wave anisotropy in the earth's inner core. *Geophysical Research Letters*, 48(19): e94784
- Wang T, Song X, Xia H H. 2015. Equatorial anisotropy in the inner part of Earth's inner core from autocorrelation of earthquake coda. *Nature Geoscience*, 8(3): 224–227
- Wang W, Li Y, Brodholt J P, Vočadlo L, Walter M J, Wu Z. 2021. Strong shear softening induced by superionic hydrogen in Earth's inner core. *Earth and Planetary Science Letters*, 568: 117014
- Waszek L, Deuss A. 2011. Distinct layering in the hemispherical seismic velocity structure of Earth's upper inner core. *Journal of Geophysical Research*, 116(B12): B12313
- Waszek L, Deuss A. 2013. A low attenuation layer in the Earth's uppermost inner core. *Geophysical Journal International*, 195(3): 2005–2015
- Waszek L, Irving J, Deuss A. 2011. Reconciling the hemispherical structure of Earth's inner core with its super-rotation. *Nature Geoscience*, 4(4): 264–267
- Wen L X, Niu F L. 2002. Seismic velocity and attenuation structures in the top of the Earth's inner core. *Journal of Geophysical Research (Solid Earth)*, 107(B11): 2273
- 温联星, 田冬冬, 姚家园. 2018. 地球内核及其边界的结构特征和动力学过程. *地球物理学报*, 61(3): 803–818 [Wen L X, Tian D D, Yao J Y. 2018. Seismic structure and dynamic process of the Earth's inner core and its boundary. *Chinese Journal of Geophysics*, 61(3): 803–818 (in Chinese with English abstract)]
- Woodhouse J H, Giardini D, Li X D. 1986. Evidence for inner core anisotropy from free oscillations. *Geophysical Research Letters*, 13(13): 1549–1552
- Wookey J, Helffrich G. 2008. Inner-core shear-wave anisotropy and texture from an observation of PKJKP waves. *Nature*, 454(7206): 873–876
- Yang Y, Song X. 2020. Temporal changes of the inner core from globally distributed repeating earthquakes. *Journal of Geophysical Research: Solid Earth*, 125(3): e2019JB018652
- Yang Y, Song X. 2023. Multidecadal variation of the Earth's inner-core rotation. *Nature Geoscience*, 16(2): 182–187
- 杨翼, 宋晓东. 2021. 重复地震和地球内核的时变性. *地球与行星物理论评*, 52(1): 1–10 [Yang Y, Song X D. 2021. Repeating earthquakes and temporal changes of the Earth's inner core. *Reviews of Geophysics and Planetary Physics*, 52(1): 1–10 (in Chinese with English abstract)]
- Yoshida S, Sumita I, Kumazawa M. 1996. Growth model of the inner core coupled with the outer core dynamics and the resulting elastic anisotropy. *Journal of Geophysical Research: Solid Earth*, 101(B12): 28085–28103
- Yu W C, Wen L X. 2006. Seismic velocity and attenuation structures in the top 400 km of the Earth's inner core along equatorial paths. *Journal of Geophysical Research (Solid Earth)*, 111(B7): B07308
- Yu W C, Wen L X. 2007. Complex seismic anisotropy in the top of the Earth's inner core beneath Africa. *Journal of Geophysical Research (Solid Earth)*, 112(B8): B08304
- Zhang J, Song X D, Li Y C, Richards P G, Sun X, Waldhauser F. 2005. Inner core differential motion confirmed by earthquake waveform doublets. *Science*, 309(5739): 1357–1360

(本文责任编辑: 刘莹; 英文审校: 张兴春)

特约主题信息

【编者按】侯德封矿物岩石地球化学青年科学家奖从设立至今已历经38年,举办了19届。从最初的每届表彰人数不超过6人,到现今每届不超过20人,参评候选人逐年递增,且其成果越来越丰富;同时获奖者在各自的专业领域为科技创新做出贡献,很多已成长为学科带头人和各单位的中坚。侯德封奖以成果的创新性为第一原则,坚持公平、公开和公正的原则,为发现人才、培养人才做出的努力,赢得了社会各界的广泛赞赏和肯定,其关注度和认可度与日俱增。2023年2月17日,学会侯德封奖评选工作委员会在北京召开了第19届评审会,经预审、综合评议和无记名投票,最后评选出20名获奖人。为了宣传获奖人的成果,本刊特辟“侯德封奖获奖者论文”栏目刊载获奖人的学术论文,以飨读者。本期刊发第19届侯德封奖获奖人欧阳荷根、何宇、柏中杰、王华建、胡清扬的论文。

作者简介

欧阳荷根,1984年生,中国地质科学院矿产资源研究所研究员,博士生导师。主要从事斑岩-矽卡岩型铜矿和钼矿、与高分异花岗岩有关钨锡矿以及岩浆-热液型铅锌银矿的成矿机制和找矿勘查研究。在*Economic Geology, SEG Special Publication, American Mineralogist*等期刊发表论文40余篇,论文总引用1520余次。获第19届侯德封矿物岩石地球化学青年科学家奖。现任中国地质学会矿床专业委员会委员,《地质通报》青年编委。



何宇,中国科学院地球化学研究所研究员,2012年获得中国科学院大学凝聚态物理博士学位,建立了第一性原理计算研究平台,从事高温高压下地球内部物质性质的第一性原理研究,研究地球内部固态离子输运和超离子态。获得第19届侯德封青年科学家奖和2022年中国十大新锐科技人物。目前以第一/通信作者在*Nature, Nat. Geosci., Nat. Commun., National Science Review*等国际知名期刊上发表SCI文章18篇,有两篇文论入选ESI高被引论文,总引用1000余次。

